Transport of Intensity Equation Method and its Applications

Masanori Mitome

1-1 Namiki Tsukuba Ibaraki, International Center for Materials Nanoarchitectonics, National Institute for Materials Science

Tel: +81-29-860-4431

FAX: +81-29-851-6280

e-mail: MITOME.Masanori@nims.go.jp

Running title: TIE method and its applications

Key words: Transport of intensity equation, Phase retrieval, Boundary conditions, Quantitative measurements

Abstract

A phase retrieval technique based on a transport of intensity equation (TIE) is one of the defocus series reconstruction techniques in microscopy. Since it does not require any dedicated devices like a biprism, and only three defocus images are enough to retrieve phase information, it has been applied to observe magnetic fields, magnetic domains, electrostatic potentials, and strains. It is also used to improve image resolution by correcting spherical aberration. This technique is simple and easy to use, but some artifacts often appear in the retrieved phase map. One should pay careful attention to the experimental conditions, and the algorithms and boundary conditions used to solve the TIE. This paper reviews the principle of the TIE method, the algorithms used to solve it, and application results in materials science.

1. Introduction

Phase retrieval has been a very significant but hard problem to solve in microscopy, and many kinds of techniques have ever been proposed. Those that require some images taken at different defocuses to recover phase information are categorized as defocus series reconstruction techniques. They are also sometimes referred to as inline holography, in comparison to off-axis holography in which a biprism is used to interfere an object wave and a reference wave [1]. A technique based on a transport of intensity equation (TIE) reviewed in this paper is one of the inline holography techniques.

The most characteristic feature of the TIE method is that the number of required images is very few compared to the other inline holography techniques, a maximum likelihood method (MAL) [2, 3], focal-tilt series restoration (FTSR) [4, 5], or iterative wave function reconstruction (IWFR) [6]. The TIE method usually requires only three defocus images to retrieve phase, and two images are enough in some cases. Furthermore, some popular solvers do not require an iterative calculation, and a phase map can be evaluated very quickly by use of the fast Fourier transform

(FFT) [7].

On the other hand, some artifacts often appear in phase maps retrieved by the TIE method [8]. The artifacts depend on the exact nature of the algorithms and boundary conditions to solve the TIE, and there are some controversies about quantitative reliability of phase retrieved by the TIE method [1].

In the next section, the TIE is derived from a simple Helmholtz equation and it is shown that the TIE is a universal equation for every wave. Solution algorithms and boundary conditions are described with a discussion about the artifacts in the third section. Some applications in a material science field are then introduced in the fourth section. General characteristics of the TIE are summarized in the final section.

2. Derivation of TIE

To derive the TIE we start from a simple Helmholtz equation as follows,

$$(\nabla^2 + k^2)\psi(\mathbf{r}) = 0. \quad (1)$$

Here k is a wave vector. Every wave that propagates in free space could be

described by a Helmholtz equation, and thus the following derivation is valid not only for electron waves but also for light, X-rays and so on. A wave function $\psi(\mathbf{r})$ can be represented as follows without any loss of generality,

$$\psi(\mathbf{r}) = u(\mathbf{r}_\perp, z)e^{ikz}. \quad (2)$$

Here, z is an axis coordinate that a wave propagates towards and $\mathbf{r} = (\mathbf{r}_\perp, z)$. Using this expression, the Helmholtz equation can be rewritten as

$$\nabla_\perp{}^2\psi(\mathbf{r}_\perp, z) + \left(\frac{\partial^2 u(\mathbf{r}_\perp,z)}{\partial z^2} + 2ik\frac{\partial u(\mathbf{r}_\perp,z)}{\partial z}\right)e^{ikz} = 0, \quad (3)$$

where $\nabla_\perp{}^2 = \frac{\partial^2}{\partial x^2} + \frac{\partial^2}{\partial y^2}$, is a 2-dimensional Laplacian. Assuming the second derivative of u can be neglected compared to the first derivative, the next equation can be derived,

$$\left(\nabla_\perp{}^2 + 2ik\frac{\partial}{\partial z} + 2k^2\right)\psi(\mathbf{r}_\perp, z) = 0. \quad (4)$$

This is called a paraxial Helmholtz equation. The approximation introduced here is referred to in various ways in different scientific fields; a paraxial approximation, a parabolic approximation, a small angle approximation or a slowly varying envelope approximation.

The wave function may be expressed in terms of the intensity I and the phase ϕ ,

i.e.,

$$\psi(\mathbf{r}_\perp, z) = \sqrt{I(\mathbf{r}_\perp, z)}e^{i\phi(\mathbf{r}_\perp, z)}e^{ikz} \quad (5)$$

Substituting this expression into the paraxial Helmholtz equation, two equations can be derived for the real and imaginary parts. The equation for the imaginary part is written as

$$\nabla_\perp[I(\mathbf{r}_\perp, z)\nabla_\perp\phi(\mathbf{r}_\perp, z)] = -k\frac{\partial I(\mathbf{r}_\perp, z)}{\partial z}. \quad (6)$$

This equation is called the transport of intensity equation (TIE) [9]. The required condition to derive the TIE is just a paraxial approximation and it describes a quite universal property for every wave. The TIE describes a relation between the intensity I, phase ϕ and intensity derivative with respect to the wave propagation direction $\partial I/\partial z$.

The intensity distribution can be detected as images by various devices. If the intensity derivative can be estimated from some defocus images, one can retrieve the phase by solving the TIE. Since the intensity and the intensity derivative should be measured on some propagated plane that is usually an image plane, the phase retrieved by solving the TIE is on that same plane.

In a standard procedure, three images are taken with an equal defocus step (Fig. 1). A center image is considered as the intensity I on a plane in the TIE, and the images on the previous and next planes are used to estimate the intensity derivative $\partial I/\partial z$ by taking the difference of the two images. For example the intensity derivative can be estimated by a linear approximation in the following manner,

$$\frac{\partial I(\mathbf{r}_\perp,z)}{\partial z} \approx \frac{I(\mathbf{r}_\perp,z+\Delta z)-I(\mathbf{r}_\perp,z-\Delta z)}{2\Delta z}, \tag{7}$$

where Δz is axial defocus distance.

If the image contrast is quite low, the center image could be estimated by the mean of two images on neighboring planes. In this case, two images are enough to retrieve phase information.

To simplify the TIE, intensity I is assumed to be constant. It is a very rough approximation but it is helpful to understand the TIE properties. Under this approximation the intensity in the TIE can be extracted from the gradient operator, and the TIE is simplified as

$$\nabla_\perp{}^2\phi(\mathbf{r}_\perp,z) = -\frac{k}{I}\frac{\partial I(\mathbf{r}_\perp,z)}{\partial z}. \tag{8}$$

This means that curvature of a phase map is proportional to the derivative of the

normalized intensity and the TIE is related to the Huygens-Fresnel principle [10].

The principle of the TIE method is simple, but some artifacts often appear in the phase maps retrieved by the TIE method [8]. The artifacts depend on the evaluation algorithms and boundary conditions used to solve the TIE which are described in the next section.

3. Algorithms to solve TIE and boundary conditions

3-1. Dirichlet boundary condition

The TIE is a second order partial differential equation, and thus some boundary condition is necessary to solve it. In the original paper by Teague [9], a Green's function is used to solve the TIE with Dirichlet boundary conditions. In the Dirichlet boundary conditions one need to know a phase function on a boundary a priori, but it is usually difficult to measure it experimentally. Thus, this evaluation algorithm is rarely used in experiments.

3-2. Periodic boundary condition and FFT

To avoid the difficulties of the Dirichlet boundary conditions, some researchers proposed to use periodic boundary conditions and a fast Fourier transform (FFT) to solve the TIE [7, 11, 12]. A plug-in software for Gatan DigitalMicrograph based on the FFT has been released commercially [13].

To solve the TIE an intermediate function Φ is introduced here as follows [9],

$$\nabla_\perp \Phi(\mathbf{r}_\perp, z) = I(\mathbf{r}_\perp, z) \nabla_\perp \phi(\mathbf{r}_\perp, z). \tag{9}$$

The TIE can be rewritten as the following Poisson's equation,

$$\nabla_\perp{}^2 \Phi(\mathbf{r}_\perp, z) = -k \frac{\partial I(\mathbf{r}_\perp, z)}{\partial z}. \tag{10}$$

For the intermediate function Φ the other Poisson's equation can be obtained as

$$\nabla_\perp{}^2 \phi(\mathbf{r}_\perp, z) = \nabla_\perp \left\{ \frac{1}{I(\mathbf{r}_\perp, z)} \nabla_\perp \Phi(\mathbf{r}_\perp, z) \right\}. \tag{11}$$

A formal solution for phase can be written as following with use of an inverse Laplacian operator $\nabla_\perp{}^{-2}$,

$$\phi(\mathbf{r}_\perp, z) = -k \nabla_\perp{}^{-2} \nabla_\perp \left\{ \frac{1}{I(\mathbf{r}_\perp, z)} \nabla_\perp \nabla_\perp{}^{-2} \frac{\partial I(\mathbf{r}_\perp, z)}{\partial z} \right\}. \tag{12}$$

The inverse Laplacian operator can be expressed by a combination of Fourier transform and inverse Fourier transform as [12, 14]

$$\nabla_\perp{}^{-2} = -F^{-1} \frac{1}{q^2} F. \tag{13}$$

Here F and F^{-1} are a Fourier transform operator and an inverse Fourier transform operator, and q denotes reciprocal coordinate.

From equation (13), the frequency characteristics of the TIE method can be perceived. Dividing by a reciprocal coordinate means that higher frequency components of phase ϕ are involved intensely in the intensity derivative $\partial I/\partial z$, whereas lower frequency components are faintly in it. In order to retrieve the lower frequency components of phase, one needs to measure the lower frequency components of the intensity derivative precisely and distinctly with high signal to noise ratio. Otherwise, the inverse Laplacian operator amplifies the low frequency noise in images unnecessarily and fails to retrieve the lower frequency components of phase [8].

To measure the lower frequency components of intensity derivative distinctly, it is better to use a longer defocus distance Δz in equation (7). However, a long defocus distance deteriorates the estimation accuracy of the intensity derivative in equation (7). It has been discussed how long defocus distance is acceptable in the estimation of the intensity derivative by a Fourier analysis [14], and resulted in following,

$$2\Delta z \leq \frac{2.45}{\pi\lambda {q_{\max}}^2}, \quad (14)$$

where λ is a wavelength and $q_{\max}$ is the required highest spatial frequency component in a phase map.

Some researchers have proposed to use a regularization [14, 15] to avoid divergence at $q = 0$ in equation (13) or band pass filters to reduce the lower frequency noise [16]. One example is a Tikhonov's regularization where $1/q^2$ in equation (13) is replaced by $q^2/(q^2+q_c^2)^2$ with a constant parameter q_c. Taking a higher value of the parameter q_c suppresses the low frequency noise effectively, but quantitative quality of the phase map deteriorates when the q_c is too large. To keep the phase map quantitative, this parameter should be chosen adequately to represent the frequency components composing in an observed object [17].

3-3. Neumann condition and discrete cosine transfer (DCT)

Low frequency artifacts that appear in phase maps retrieved by using a periodic boundary condition have been pointed out by some researchers, and they proposed to use Neumann boundary conditions instead.

Volkov *et al.* proposed to extend an experimental image by flipping it vertically and horizontally and joining them together as in Fig. 2 [18]. They used FFT to solve the TIE for the expanded images. This procedure makes the Neumann boundary condition valid virtually, but the intensity conservation low is invalid on the virtual boundary. The TIE should be explicitly assumed the intensity conservation low [19], and thus the procedure proposed by Volkov *et al.* still causes some artifacts.

Zho *et al.* proposed to insert a hard-edged aperture to make the Neumann boundary condition actually on the aperture edge, and use a discrete cosine transfer (DCT) to solve the TIE [20, 21]. The DCT technique has been improved by using an iterative calculation (iDCT) to extend the technique to arbitrarily shaped apertures [22]. Ishizuka *et al.* also proposed to use a selected area aperture to make the Neumann boundary condition and they used the iDCT to solve the TIE [23]. In these experiments, the Neumann boundary condition is actually valid by inserting the hard apertures and the energy conservation low is also valid on the boundary. Consequently, artifacts are considerably reduced.

3-4. Hybrid algorithm

Koch *et al.* combined some ideas to avoid artifacts seen in phase maps and proposed a hybrid algorithm which they named a full-resolution wave reconstruction (FRWR) [1, 24]. They proposed some improvements in the algorithm; (1) a large defocus range to recover lower frequency information, (2) non-linear sampling of defocus values to recover not only low-frequency, but also high-frequency, information, (3) incremental inclusion of images to align images taken in different defocus, (4) distortion correction to compensate magnification difference, rotation and distortion in images, (5) padding to remove artifacts due to aperiodicity, and (6) phase prediction to make convergence of an iterative calculation faster. They distributed a plug-in software for DigitalMicrograph on a web page [25].

4. Applications

4-1. Magnetic field

Phase retrieval techniques are often used to observe magnetic fields or magnetic domains because the phase is sensitive to the fields whereas the intensity is little

influenced by them. The TIE method is convenient to image the fields in magnetic materials since it does not require any additional devices.

Ishizuka *et al.* reported observation results of magnetic domains seen in Perovskite-type manganese tri-oxide $Pr_{1-x}(Ca_{1-y}, Sr_y)_xMnO_3$ (x=0.45, y=0.4) by Lorentz transmission electron microscope (LTEM) and the TIE method [26]. The domain structure is clearly observed and the magnetization directions are seen with a color wheel like in Fig. 3.

Yu *et al.* succeeded to observe a two-dimensional skyrmion in $Fe_{0.5}Co_{0.5}Si$ using LTEM and the TIE method [27]. They showed that skylmions form a hexagonal arrangement of swirling spin textures and they are stable over a wide range of the phase diagram (Fig. 4). The TIE method can reveal dynamic behaviors like motions of vortices, domain walls and skyrmions spanning with time resolution of a few to ten seconds, but quantitative analysis is sometimes unreliable because of the artifacts. Off-axis electron holography has been used for the quantitative analysis of the skylmions [28, 29], and a linear relationship between phase shifts and a sample thickness has been revealed as $\varphi = 0.00173t$ for thickness less than 500 nm [28].

Kohn *et al.* evaluated the quantitative magnetic phase reconstructions for $Ni_{80}Fe_{20}$ (Permalloy) particles [30]. They concluded that quantitative reconstructions for the magnetic elements were achieved at a defocus range between 200 μm and 800 μm. It is important to choose a defocus adequately in order to keep the phase map quantitative.

The phase of electron waves is shifted by not only magnetic fields but also by electrostatic fields. Humphrey *et al.* proposed a revised formalism of the TIE to separate magnetic and electrostatic components [31]. They tested the formalism experimentally by observing a CoFeB amorphous film.

Kashyap *et al.* reported observation results of near-eutectoid Co-Pt alloys [32]. They observed a nano-chessboard pattern in dark field images and reported that the chessboard structure revealed a zig-zag shaped magnetic domain wall.

Tamura *et al*. observed magnetic bubbles by Lorentz microscopy and compared the magnetization maps obtained by MAL method and TIE method [33]. They described that the results obtained by MAL method is more reliable and precise than those obtained by TIE method. The MAL method usually requires typically 20 or

more defocus images and 10 to 20 iterative calculation to obtain optimum results. On the other hand, TIE requires only a few images and do not need an iterative calculation typically. TIE is easy and fast to estimate phase maps though they are less reliable quantitatively.

4-2. Potential imaging

Electron waves are also influenced from inner potential in materials, and thus the TIE method has been applied to image a potential map. Petersen *et al.* observed a p-n junction in a silicon wafer [34], Au nanospheres [35] and MgO nano-cubes [36]. Takahashi *et al.* succeeded to image the potential gradient on Pt induced by hydrogen adsorption [37]. They concluded that the potential gradient was localized at Pt interfaces.

4-3. Strain mapping

The TIE method can be also applied to a strain mapping. Song *et al.* applied it to image strain in a light emitting diode [38]. They succeeded to image a strain map in

GaN/InGaN multiple quantum wells. They also pointed out that phase maps retrieved with a FFT algorithm are noisier than those obtained by the iterative approach proposed by Koch [24].

4-4. High resolution imaging

The phase retrieved by the TIE method is usually that on an image plane, because the intensity I and the intensity derivative $\partial I/\partial z$ in the TIE (equation (6)) are measured on an image plane and thus the phase ϕ itself is also obtained on the image plane. Since it is known that the propagation behavior of waves in an objective lens can be described by a transfer function with a spherical aberration coefficient of the objective lens, it is possible to back-propagate the wave from the image plane until it reaches the specimen exit plane. Furthermore, one can correct the aberration effects and improve the resolution in images. Ishizuka *et al.* showed an aberration corrected high resolution image of Si_3N_4 can be obtained from the phase information retrieved by the TIE method [14].

Zhang *et al.* applied the TIE method to high resolution images of MoS_2 taken with

an aberration corrected transmission electron microscope [39]. They used a small defocus difference of 12 to 20 nm to retrieve the higher frequency components and reported that the phase difference between a single molybdenum atom column and a double sulfur column can be measured quantitatively as 0.01 rad.

5. Conclusion

This paper reviewed the TIE method to retrieve phase information. It usually needs only three images taken at different defocus values and does not require any additional devices like as a biprism. It is easy and simple to apply to experimental images taken by existing microscopes.

On the other hand, one should pay attention to the experimental conditions, e.g. defocus distance in taking defocus images and magnification. Otherwise, artifacts can appear in the phase map and worsen the results. Furthermore, one needs to choose an appropriate algorithm to solve the TIE according to the boundary conditions. Although there are some complicated issues to consider, it is worthwhile to attempt a TIE approach first when one needs to obtain phase information.

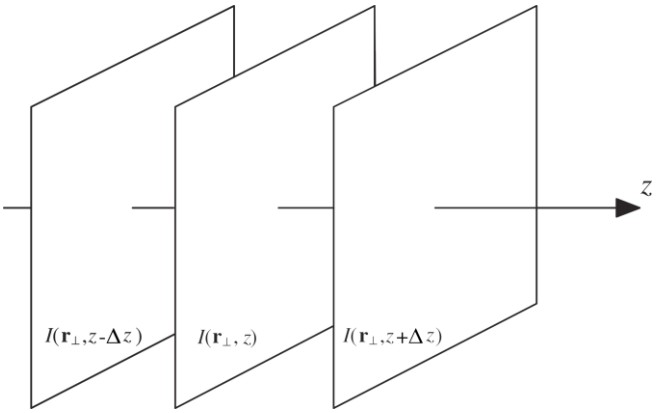

Fig. 1 A standard procedure to take defocus images for retrieving phase by the TIE method. *Z* indicates the wave propagation direction.

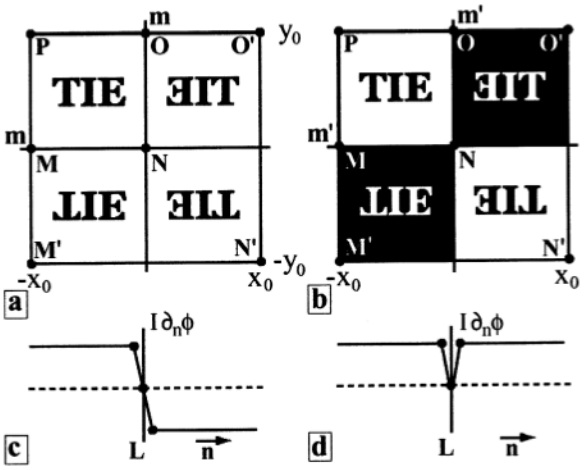

Fig. 2 Even (a) and odd (b) symmetric extensions of an original image satisfying the internal TIE symmetry and a Neumann boundary condition. Reprinted by permission from Elsevier [18], Copyright (2002).

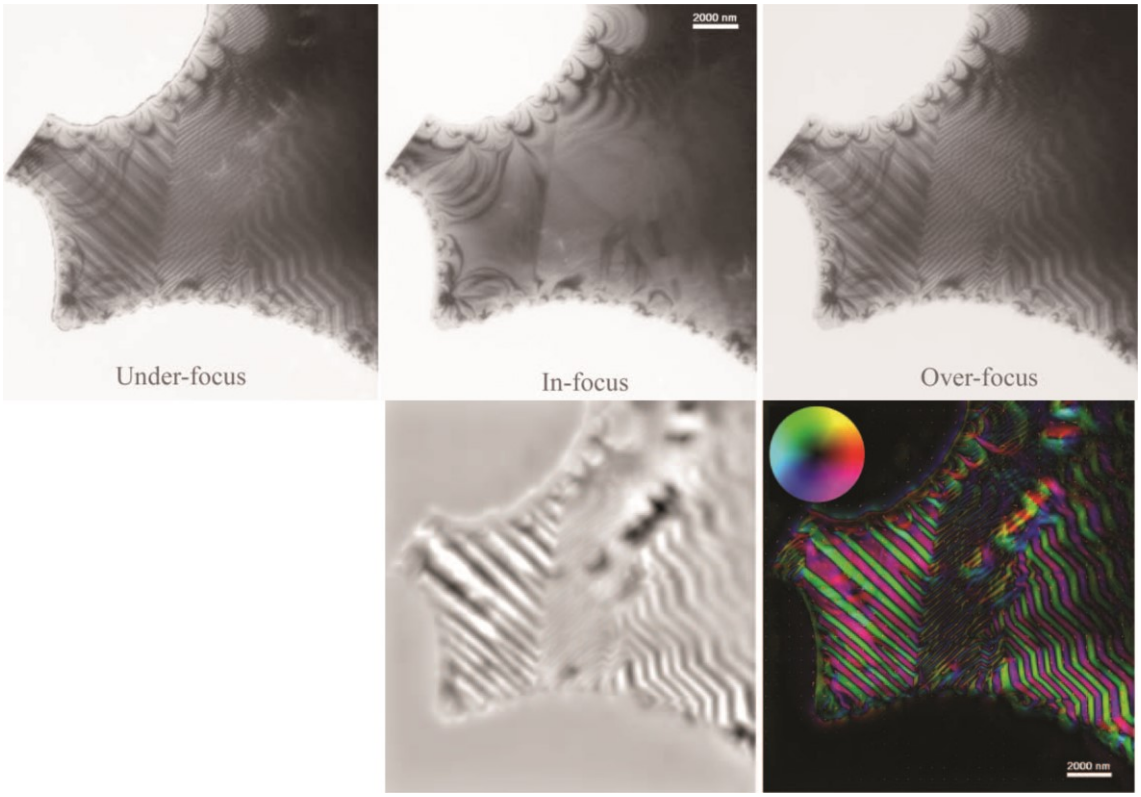

Fig. 3 Defocus images of Perovskite-type manganese tri-oxide $Pr_{1-x}(Ca_{1-y}, Sr_y)_xMnO_3$ (x=0.45, y=0.4) taken by a Lorentz microscope (upper 3 images). A phase map retrieved by the TIE method from upper 3 images (lower middle), and a magnetization vector map (lower right).
Reprinted by permission from Cambridge University Press [26], Copyright (2005).

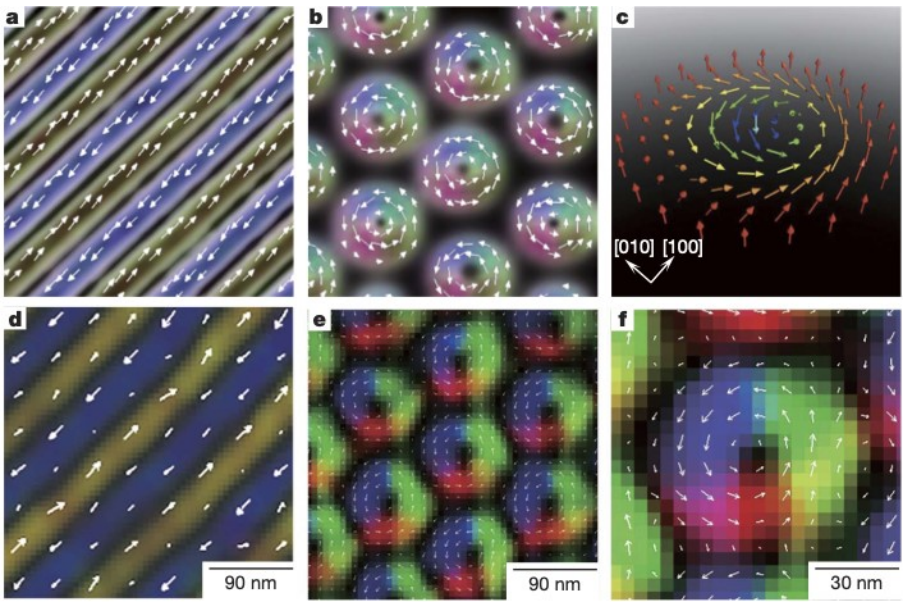

Fig. 4 Topological spin textures in the helical magnet $Fe_{0.5}Co_{0.5}Si$.
Helical (a) and skyrmion (b) structures predicted by Monte Carlo simulation.
(d)-(f) shows experimental results.
Reprinted by permission from Nature [27], Copyright (2010).

References

[1] Koch C T, and Lubk A (2010) Off-axis and inline electron holography: A quantitative comparison. *Ultramicroscopy* **110**, 460–471.
[2] Coene W M J, Thust A, Op de Beeck M and Van Dyck D (1996) Maximum-likelihood method for focus-variation image reconstruction in high resolution transmission electron microscopy. *Ultramicroscopy* **64**, 109–135.
[3] Thust A, Coene W M J, Op de Beeck M and Van Dyck D (1996) Focal-series reconstruction in HRTEM: simulation studies on non-periodic objects. *Ultramicroscopy* **64**, 211–230.
[4] Meyer R R, Kirkland A I and Saxton W O (2002) A new method for the determination of the wave aberration function for high resolution TEM. 1. Measurement of the symmetric aberrations. *Ultramicroscopy* **92**, 89–109.
[5] Meyer R R, Kirkland A I, and Saxton W O (2004) A new method for the determination of the wave aberration function for high-resolution TEM. 2. Measurement of the antisymmetric aberrations. *Ultramicroscopy* **99**, 115–123.
[6] Allen L J, McBride W, O'Leary N L, and Oxley M P (2004) Exit wave reconstruction at atomic resolution. *Ultramicroscopy* **100**, 91–104.
[7] Paganin D, and Nugent K A (1998) Noninterferometric Phase Imaging with Partially Coherent Light. *Phys. Rev. Lett.* **80**, 2586–2589.
[8] Paganin D, Barty A, McMahon P J, and Nugent K A (2004) Quantitative phase-amplitude microscopy. III. *J. Microsc.* **214**, 51–61.
[9] Teague M R (1983) Deterministic phase retrieval: a Green's function solution. *J. Opt. Soc. Am.* **73**, 1434-1441.
[10] Streibl N (1984) Phase imaging by the transport equation of intensity. *Opt. Commun.* **49**, 6–10.
[11] Gureyev T E, and Nugent K A (1997) Rapid quantitative phase imaging using the transport of intensity equation. *Opt. Commun.* **133**, 339–346.
[12] Allen L J, and Oxley M P (2001) Phase retrieval from series of images obtained by defocus variation. *Opt. Commun.* **199**, 65–75.
[13] https://www.hremresearch.com/Eng/plugin/QPtEng.html
[14] Ishizuka K, and Allman B (2005) Phase measurement of atomic resolution image using transport of intensity equation. *J. Electron Microsc.* **54**, 191–197.
[15] Gureyev T E, Pogany A, Paganin D M, and Wilkins S W (2004) Linear algorithms for phase retrieval in the Fresnel region. *Opt. Commun.* **231**, 53–70.
[16] Komuro K, and Nomura T (2016) Quantitative phase imaging using transport of intensity equation with multiple bandpass filters. *Appl. Opt.* **55**, 5180-5186.
[17] Mitome M, Ishizuka K, and Bando Y (2010) Quantitativeness of phase measurement by transport of intensity equation. *J. Electron Microsc.* **59**, 33–41.
[18] Volkov V V, Zhu Y, and De Graef M (2002) A new symmetrized solution for phase retrieval using the transport of intensity equation. *Micron* **33**, 411–416.
[19] Teague M R (1982) Irradiance moments: their propagation and use for unique retrieval of phase. *J. Opt. Soc. Am.* **72**, 1199-1209.
[20] Zuo C, Chen Q, and Asundi A (2014) Boundary-artifact-free phase retrieval with the transport of intensity equation: fast solution with use of discrete cosine transform. *Opt. Express* **22**, 9220-9224.
[21] Zuo C, Chen Q, Li H, Qu W, and Asundi A (2014) Boundary-artifact-free phase

retrieval with the transport of intensity equation II: applications to microlens characterization. *Opt. Express* **22**, 18310-18324.
[22] Huang L, Zuo C, Idir M, Qu W, and Asundi A (2015) Phase retrieval with the transport-of-intensity equation in an arbitrarily shaped aperture by iterative discrete cosine transforms. *Opt. Lett.* **40**, 1976-1979.
[23] Ishizuka A, Mitsuishi K, and Ishizuka K (2018) Direct observation of curvature of the wave surface in transmission electron microscope using transport intensity equation. *Ultramicroscopy* **194**, 7–14.
[24] Koch C T (2014) Towards full-resolution inline electron holography. *Micron* **63**, 69–75.
[25] https://www.physics.hu-berlin.de/en/sem/software
[26] Ishizuka K, Allman B (2005) Phase Measurement in Electron Microscopy Using the Transport of Intensity Equation. *Micros. Today* **13**, 22-25.
[27] Yu X Z, Onose Y, Kanazawa N, Park J H, Han J H, Matusi Y, Nagaosa N, and Tokura Y (2010) Real-Space Observation of a Two-Dimensional Skyrmion Crystal. *Nature* **465**, 901–904.
[28] Park H S, Yu X, Aizawa S, Tanigaki T, Akashi T, Takahashi Y, Matsuda T, Kanazawa N, Onose Y, Shindo D, Tonomura A, and Tokura Y (2014) Observation of the magnetic flux and three-dimensional structure of skyrmion lattices by electron holography. *Nat. Nanotechnol.* **9**, 337–342.
[29] Kovács A, Li Z A, Shibata K, and Dunin-Borkowski R E (2016). Lorentz microscopy and off-axis electron holography of magnetic skyrmions in FeGe. *Resolution and Discovery* **1**, 2–8.
[30] Kohn, A, Habibi A, and Mayo M (2016) Experimental Evaluation of the 'Transport-of-Intensity' Equation for Magnetic Phase Reconstruction in Lorentz Transmission Electron Microscopy. *Ultramicroscopy* **160**, 44–56.
[31] Humphrey E, Phatak C, Petford-Long A K, and De Graef M (2014) Separation of Electrostatic and Magnetic Phase Shifts Using a Modified Transport-of-Intensity Equation. *Ultramicroscopy* **139**, 5–12.
[32] Kashyap I, Vetter E P, Floro J A, and De Graef M (2019) Lorentz TEM Study of the Magnetic Microstructure in Near-Eutectoid Co-Pt Alloys. *J. Magne. and Magnetic Mater.* **479**, 204–11.
[33] Tamura T, Nakane Y, Nakajima H, Mori S, Harada K and Takai Y (2018) Phase retrieval using through-focus images in Lorentz transmission electron microscopy. *Microscopy* **67**, 171–177.
[34] Petersen T C, Keast V J, Johnson K, and Duvall S (2007) TEM-based phase retrieval of p–n junction wafers using the transport of intensity equation. *Philos Mag.* **87**, 3565-3578.
[35] Petersen T C, Bosman M, Keast V J, and Anstis G R (2008) Plasmon resonances and electron phase shifts near Au nanospheres. *Appl. Phys. Lett.* **93**, 101909.
[36] Petersen T C, Keast V J, and Paganin D M (2008) Quantitative TEM-based phase retrieval of MgO nano-cubes using the transport of intensity equation. *Ultramicroscopy*. **108**, 805-815.
[37] Takahashi Y, Kasai H, and Usagawa T (2017) Imaging of potential gradient on platinum induced by hydrogen adsorption. *Appl. Phys. Lett*. **111**, 011602.
[38] Song K, Shin G-Y, Kim J K, Oh S H, and Koch C T (2013) Strain mapping of LED

devices by dark-field inline electron holography: Comparison between deterministic and iterative phase retrieval approaches. *Ultramicroscopy* **127**, 119-125.

[39] Zhang X, and Oshima Y (2016) Atomic resolved phase map of monolayer MoS_2 retrieved by spherical aberration-corrected transport of intensity equation. *Microscopy* **65**, 422–428.